

Proceedings of the Eurosensors XXIII conference

Highly Efficient Energy Extraction from Piezoelectric Generators

T. Hehn^{a*}, F. Hagedorn^a, Y. Manoli^{a,b}^a*Department of Microsystems Engineering – IMTEK, University of Freiburg, Georges-Koehler-Allee 102, 79110 Freiburg, Germany*^b*HSG-IMIT – Institute of Micromachining and Information Technology, Wilhelm-Schickard-Straße 10, 78052 Villingen-Schwenningen, Germany*

Abstract

Active non-linear circuits with an inductor as temporary energy storage are used to increase the power output of piezoelectric microgenerators. The losses in parasitic resistances inside these circuits cause efficiencies lower than 100%. This paper presents an optimized switching technique which reduces these losses. By means of simplified approximation equations, it can be shown that independently of the system parameters, the improved switching technique has a higher efficiency than the formerly used technique, independently on the system parameters. With the parameters extracted from simulations of a CMOS integrated implementation, the efficiency can be increased by 9%.

Keywords: Energy harvesting ; piezoelectric microgenerators ; conversion circuits ; energy extraction

1. Introduction

Piezoelectric microgenerators (PZTs) are suitable for harvesting ambient vibration energy in order to supply low-power electronic devices like wireless sensor nodes. Since power is discontinuously produced only when there is vibration, a storage element, e.g. a large capacitor or a battery, is usually charged by the PZT, and the electronic device is powered by the storage element. An interface or conversion circuit connected between the PZT and the storage element can increase the PZT output power, compared to using a direct connection¹. These conversion circuits commonly use an inductor as temporary energy storage, and the energy flow between the PZT, the inductor and the storage element is managed by several switches. In reality, the efficiency of such an interface circuit is always lower than 100% due to the losses in the parasitic series resistances of the switches, the inductor and the rectifier. The influence of these parasitic resistances on the efficiency has rarely been studied². In this paper, an improved switching technique is presented which reduces the losses in the parasitic resistances and thus increases the efficiency, compared to the switching techniques used in previous publications^{1,3}. Simplified approximated efficiency equations make a comparison of the formerly used and the improved switching technique possible. By means of these equations and additional evaluation of the approximation error, it is hypothesized that the efficiency of the improved switching technique is better, independently of the system parameters like inductor size, PZT voltage etc.

* Corresponding author. Tel.: +49-761-203-7510; fax: +49-761-203-7592.

E-mail address: thorsten.hehn@imtek.de

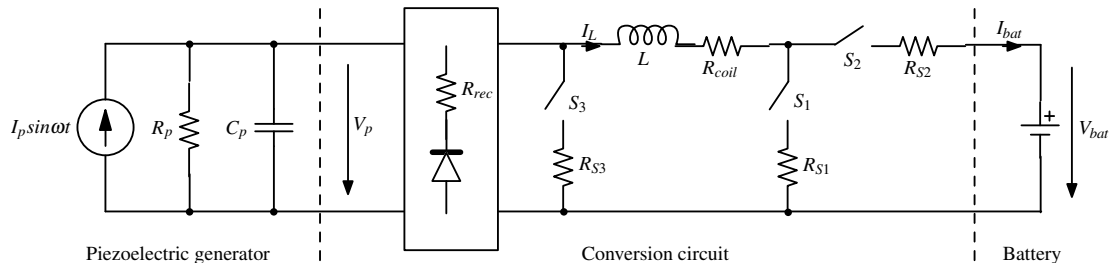


Fig. 1. Functional diagram of the energy harvesting system including parasitic series resistances. The circuit parameters are $R_p = 1.8 \text{ M}\Omega$, $C_p = 12 \text{ nF}$, $I_p = 30 \mu\text{A} \dots 180 \mu\text{A}$, $\omega = 2\pi \cdot 250 \text{ Hz}$, $L = 100 \mu\text{H}$, $V_{bat} = 2.5 \text{ V}$

2. Energy harvesting circuit and energy loss approximation

Fig. 1 shows the energy harvesting system. The PZT is modeled by an AC current source with internal impedance. First of all, the PZT voltage V_p has to be rectified in order to avoid negative voltages. The conversion circuit waits until V_p reaches a maximum and then quickly transfers the energy to the battery. During the transfer process, the inductor L acts as temporary energy storage which is charged and discharged, thus the current I_L produces losses in the parasitic series resistances. The efficiency of the transfer process is given by equation (1), where $\overline{P_{in}}$, $\overline{P_{loss}}$, E_{in} and E_{loss} are the average input power, the average power loss inside the circuit, and the corresponding energies. The length of one transfer cycle is denoted by T .

$$\eta = 1 - \frac{\overline{P_{loss}}}{\overline{P_{in}}} = 1 - \frac{E_{loss}/T}{E_{in}/T} = 1 - \frac{E_{loss}}{E_{in}} \quad (1)$$

Since the exact calculation of E_{loss} can be difficult depending on the switching technique, a simplified method is now presented. In order to calculate the energy loss $E(R, \mathbf{p})$ in an arbitrary resistance R for an arbitrary circuit parameter set \mathbf{p} , equation (2) can be used. Assuming that the current $I_R(t, R, \mathbf{p})$ through R and the duration $T_R(R, \mathbf{p})$ of the current flow are both functions of R and \mathbf{p} , it is nearly impossible to find analytic solutions of the integral $k(R, \mathbf{p})$. It is of course possible to calculate $k(R, \mathbf{p})$ numerically, but since this can only be done for one parameter set \mathbf{p} at a time, this method cannot be used to compare the energy losses for all possible parameters. A better way is to perform a first order Taylor approximation $E_{lin}(R, \mathbf{p})$ of the function $E(R, \mathbf{p})$ in equation (2) around $R = 0 \Omega$, assuming R to be small. According to the resulting equation (3), it is sufficient to calculate $k(0\Omega, \mathbf{p})$, i.e. to know the current through R for $R = 0\Omega$, which is well-known in contrast to the lossy case. Applied to the circuit shown in Fig. 1, this procedure enables direct comparison between the efficiencies of different switching techniques, under the condition that the approximation error is reasonably low.

$$E(R, \mathbf{p}) = R \cdot \int_0^{T_R(R, \mathbf{p})} I_R^2(t, R, \mathbf{p}) dt = R \cdot k(R, \mathbf{p}) \quad \text{where} \quad k(R, \mathbf{p}) := \int_0^{T_R(R, \mathbf{p})} I_R^2(t, R, \mathbf{p}) dt \quad (2)$$

$$E(R, \mathbf{p}) \approx E_{lin}(R, \mathbf{p}) := E(0\Omega, \mathbf{p}) + R \cdot \frac{\partial E}{\partial R}(0\Omega, \mathbf{p}) = R \cdot k(0\Omega, \mathbf{p}) \quad (3)$$

3. Switching techniques

The operation principle of the formerly used switching technique, called ST₁₃ in this paper, is illustrated in Fig. 2(a). In phase 1, all switches are *off*, thus the PZT capacitor C_p is charged without any losses caused by a load. After the PZT voltage V_p has reached a maximum voltage V_{p0} , the circuit changes to switch configuration SC₁ (S_1 *on*), initiating the transfer process with phase 2. During this phase, the energy $E_{in} = E_{C0} = 0.5 C_p V_{p0}^2$ stored on C_p is transferred into the inductor L . After this process has been finished, the switches change to SC₃ (S_2 and S_3 *on*, S_1 *off*). Hence, during phase 3, the energy is finally transferred into the battery. When the transfer process has

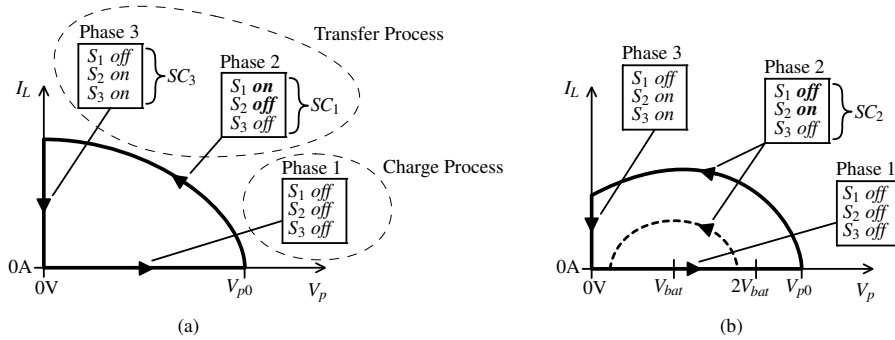


Fig. 2. State diagrams of the switching techniques ST₁₃ (a) and ST₂₃ (b). The difference between both techniques is the switch configuration in phase 2. The dashed line in (b) illustrates that energy is remaining in C_p if $V_{p0} < 2V_{bat}$.

completed, S_2 and S_3 are turned *off*, and a new cycle starts. The transfer process is shorter than the charge process by a factor of around 1000, depending on the PZT frequency, C_p and L .

The proposed technique ST₂₃ described in Fig. 2 (b) differs from ST₁₃ only in phase 2: The switches change to SC₂ (S_2 on, S_1 and S_3 off) instead of SC₃ and thus E_{C0} is carried into L and the battery simultaneously. Unlike ST₁₃ where V_{p0} is allowed to be any voltage, ST₂₃ works most efficiently if $V_{p0} > 2V_{bat}$, because otherwise energy remains in C_p at the end of phase 2 (dashed line). In order to cover the whole voltage range, ST₁₃ for $V_{p0} < 2V_{bat}$ and ST₂₃ for $V_{p0} > 2V_{bat}$ can be combined; the resulting switching technique is called ST₁₃₂₃.

It is now described how the approximated efficiencies are calculated. Each switching technique ST_{*a3*} is defined by two consecutive switch configurations SC_{*a*} and SC₃, where $a \in \{1, 2\}$. The parasitic resistances appearing in the current path I_L of each switch configuration SC_{*n*} are summed up in R_n , where $n \in \{1, 2, 3\}$. The R_n -values are summarized in Table 1. The total energy loss during the transfer process is the sum of the energy losses during phases 2 and 3. Performing the approximation according to equation (3) and putting the result into equation (1), the approximated efficiency of ST_{*a3*} can be written according to equation (4). To simplify matters, the argument $(0\Omega, p)$ is omitted; e.g. $k_{a,a3} = k_{a,a3}(0\Omega, p)$. The k -values have been calculated according to equation (2) by solving analytically the differential equations for I_L in each switch configuration; the result is summarized in Table 2. In order to evaluate which one of the two presented switching techniques is better, the difference between the approximated efficiencies of ST₂₃ and ST₁₃ is determined according to equation (5). By insertion of the appropriate equivalent series resistances from Table 1, the k -coefficients are calculated as shown in (6).

$$\eta_{a3,lin} = 1 - \frac{E_{loss,lin,a}}{E_{C0}} - \frac{E_{loss,lin,3}}{E_{C0}} = 1 - R_a \frac{k_{a,a3}}{E_{C0}} - R_3 \frac{k_{3,a3}}{E_{C0}} \quad \text{where } a \in \{1, 2\} \quad (4)$$

$$\Delta\eta_{lin} = \eta_{23,lin} - \eta_{13,lin} = \frac{1}{E_{C0}} (R_{rec} k_{rec} + R_{coil} k_{coil} + R_{S1} k_{S1} + R_{S2} k_{S2} + R_{S3} k_{S3}) \quad (5)$$

$$k_{rec} = k_{1,13} - k_{2,23}; k_{coil} = k_{1,13} + k_{3,13} - k_{2,23} - k_{3,23}; k_{S1} = k_{1,13}; k_{S2} = k_{3,13} - k_{2,23} - k_{3,23}; k_{S3} = k_{3,13} - k_{3,23} \quad (6)$$

Table 1: Equivalent parasitic series resistances for each switch configuration (see Fig. 1 and Fig. 2).

Switch configuration	Equivalent series resistance
SC ₁	$R_1 = R_{rec} + R_{coil} + R_{S1}$
SC ₂	$R_2 = R_{rec} + R_{coil} + R_{S2}$
SC ₃	$R_3 = R_{S3} + R_{coil} + R_{S2}$

Table 2: Calculated k -values from equation (4) for ST₁₃ and ST₂₃. Within the expressions: $x = V_{p0}/V_{bat}$

ST ₁₃	ST ₂₃
$k_{1,13} = E_{C0} \sqrt{\frac{C_p}{L}} \cdot \frac{\pi}{2}$	$k_{2,23} = E_{C0} \sqrt{\frac{C_p}{L}} \left\{ \left(1 - \frac{1}{x}\right)^2 \arccos \frac{1}{1-x} + \frac{1}{x} \sqrt{1 - \frac{2}{x}} \right\}$
$k_{3,13} = E_{C0} \sqrt{\frac{C_p}{L}} \cdot \frac{2}{3} x$	$k_{3,23} = E_{C0} \sqrt{\frac{C_p}{L}} \cdot \frac{2}{3} x \left(1 - \frac{2}{x}\right)^{\frac{3}{2}}$

Table 3: Parasitic resistances used for the calculated efficiency curves. All except R_{coil} are extracted from simulation by averaging U_{DS}/I_{DS} over the relevant phase. A constant PZT current $I_p = 180\mu A$ ($x = 7$) has been set.

	ST ₁₃	ST ₂₃
R_{S1}	2.0 Ω	–
R_{S2}	3.6 Ω	3.3 Ω
R_{S3}	1.6 Ω	1.6 Ω
R_{rec}	1.8 Ω	3.3 Ω
R_{coil}	1 Ω	1 Ω

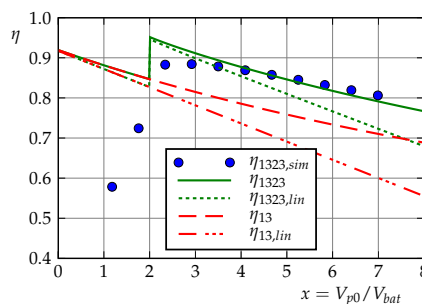


Fig. 3. Numerically solved and approximated efficiencies of ST₁₃ and ST₁₃₂₃. The used parameters are shown in Fig. 1 and Table 3. The circuit simulation results are denoted by $\eta_{1323,sim}$.

4. Results and discussion

It can be graphically shown that the k -coefficients (6) from equation (5) are positive for $x = V_{p0}/V_{bat} \geq 2$, which means that the *approximated* efficiency is higher for ST₂₃ compared to ST₁₃ for all parameters $\mathbf{p} := (C_p, L, R_{S1}, R_{S2}, R_{S3}, R_{rec}, R_{coil}, V_{p0}, V_{bat})$. In order to evaluate the approximation error and thus the quality of the approximation, the switching techniques ST₁₃ and ST₂₃ have been implemented in an integrated circuit (IC) based on a 0.35 μm CMOS technology and simulated using Cadence Spectre. The IC is powered completely by the battery; the supply voltage is $V_{bat} = 2.5$ V to ensure low-power operation. For the switches and the rectifier, high-voltage MOSFETs tolerating up to 18 V are used. Due to the large intrinsic on-resistance of these devices, the width has been set to 30 mm. Using the parasitic resistances summarized in Table 3, the exact and the approximated efficiency curves of ST₁₃₂₃ and ST₁₃ are calculated (see Fig. 3). The curves of ST₁₃₂₃ have a point of discontinuity at $x = 2$ which denotes the border between ST₁₃ and ST₂₃. The approximation error is small for $x = 0$ and $x = 2$, respectively, which denotes the lower limits of ST₁₃ and ST₂₃. The error increases for growing x and is about 8% (ST₁₃₂₃) and 11% (ST₁₃) for $x = 7$. Nevertheless, the qualitative characteristics of the exact and the approximated curves are identical.

As a conclusion of the observations described above, it can be hypothesized that not only the *approximated*, but also the overall *exact* efficiency is higher for ST₂₃ compared to ST₁₃, independently of the circuit parameters \mathbf{p} . For the specific parameter set used for the plots in Fig. 3, the exact efficiency of ST₂₃ is about 9% higher than the efficiency of ST₁₃. In order to evaluate the influence of inaccuracies of the circuit model shown in Fig. 1, efficiency values extracted from simulation at different excitation levels are shown in Fig. 3. The values have been determined by integrating $I_{bat} \cdot V_{bat}$ and dividing the result by the input energy E_{C0} . Since the circuit is powered completely by the battery, all losses caused by the IC are considered. The simulation values are in very good agreement with the exact efficiencies if $x > 2$. If $x < 2$, the constant power consumption of the controller of around 2.5 μW and the MOSFET losses dominate and thus the efficiency is drastically lower than predicted by calculations.

Acknowledgements

This work is part of the graduate program GRK 1322/1 Micro Energy Harvesting, funded by the German Research Foundation DFG (Deutsche Forschungsgemeinschaft).

References

1. Xu S et al. Low Frequency Pulsed Resonant Converter for Energy Harvesting, IEEE Trans. Power Electronics 2007; **22**:63-68
2. D'hulst R, Driesen J. Power Processing Circuits for Vibration-Based Energy Harvesters: An Integrated Approach, Proc. PowerMEMS 2008, 9-12 November, Sendai, Japan; 453-456
3. Hehn T et al. A CMOS Integrated Interface for Piezoelectric Generators, Proc. PowerMEMS 2008, 9-12 November, Sendai, Japan; 457-460